International Journal of Intelligent Knowledge Processing Systems
Vol.1, No.2, June, 2026, pp. 1-14
Journal homepage: https://ijikps.org/

COMPACT RADIO FREQUENCY FRONT-END DESIGN FOR HIGH-SPEED COMMUNICATION SYSTEMS

Suneetha Madduluri[1*], Venkata Ramani Varanasi[2]

[1] Department of Electronics and Communication Engineering, NIT Warangal, Telangana-506004, India.
(sunithasiva06@gmail.com)
[2] Department of Computer Science and Engineering, Koneru Lakshmaiah Education Foundation, Vaddeswaram-522502, Andhra Pradesh, India.
(vvramani.klu@gmail.com)

Corresponding Author Email: sunithasiva06@gmail.com

ABSTRACT

Compact, energy-saving and high-performance Radio Frequency (RF) front-end architectures are required to support the rapid development of wireless communication systems, from 5G and upcoming 6G systems through to millimeter wave systems. High gain, low noise figure, wide bandwidth, and strong linearity are all essential qualities for a conventional RF front-end design, and it is difficult to achieve all these design goals within the criteria of reduced size and low power consumption. As they become more numerous and frequent, these constraints become increasingly significant at higher operating frequencies and with growing multi-band communication needs. To tackle these challenges, this paper suggests a compact RF front-end design framework that combines multi-parameter optimization, improved impedance matching, and performance-aware architecture modeling. The proposed approach optimizes gain, noise figure, bandwidth, linearity and power efficiency all at the same time to provide balanced and stable high frequency performance. This design reduces the complexity of hardware and further improves the signal integrity, which in turn boosts the overall transmission efficiency and power efficiency. The presented compact RF front-end architecture showed better performance in various RF parameters. An overall signal classification accuracy of 99.3% was achieved, where precision stood at 98.1%, recall was 98.7%, F1 score was 98.4%, and AUC-ROC was 99.1%, signifying effective signal discrimination. The gain stability ranged from 21.4 dB to 22.5 dB in the frequency band of 2–12 GHz, whereas the noise figure ranged between 1.8 and 2.3 dB. The maximum efficiency of bandwidth for the architecture was 98.1%. The small/portable and easy to scale framework allows for adaptability to portable devices, base stations, and future wireless network deployments.

Keywords: *Bandwidth Optimization, Compact RF Front-End, High-Speed Communication Systems, Radio Frequency Design, S-Parameters, 5G Wireless Systems.*

1. INTRODUCTION

The demand for efficient and compact RF front-end architectures has risen sharply with the development of high-speed wireless communication systems like 5G, satellite communication [1], Internet of Things (IoT) and next generation Wi-Fi [2]. The modern communication system demands high data rate, low latency, low power consumption and high spectral efficiency [3]. The RF front-end, the part of the system between the antenna and the BB processing unit, is critical to the overall system performance to meet these requirements [4].

The main elements of an RF front-end are Low Noise Amplifiers (LNA), Power amplifiers (PA), Mixers, Filters, Switches and Matching Networks [5]. They should be highly efficient, stable and should minimize noise, distortion and high linearity at high frequencies and maintain the signal integrity [6]. The design of a small RF front-end, however, is not without its challenges such as parasitic effects, constraints on impedance, thermal management and potential electromagnetic interference, particularly at the microwave and millimeter-wave frequencies [7].

Recently, miniaturization and integration have become the key trends in RF front-end designs, and system-on-chip (SoC) and system-in-package (SiP) technology are highlighted [8]. High integration density and good performance are achieved with advanced semiconductor technologies like CMOS, GaN and SiGe [9]. The aim of this research is to design an optimized and compact RF front-end design for high-speed communication systems [10]. The design proposed seeks to meet the goals of better gain, noise performance [11], bandwidth efficiency and power optimization while keeping the physical footprint low [12]. The study uses these simulation and performance analyzes to study the key parameters of the compact design approach, including return loss, gain, noise figure, linearity, and power efficiency [13]. Results of this research help in the development of the next generation wireless communication system to resolve the key size-perform-power efficiency of the RF front-end design [14].

1.1 Hypothesis

H1: A compact RF front-end architecture can obtain high gain performance similar to the conventional larger size RF front-end designs.

H2: The proposed small size design will provide low noise figure for high speed communication.
H3: Linearity performance will not be significantly degraded by miniaturization of RF front-end components based on advanced semiconductor technologies (CMOS/SiGe/GaN).
H4: The front-end design will be compact and will exhibit power savings over traditional discrete component-based designs.
H5: The optimized compact RF front-end will be used for high data rate transmission for 5G and future communication systems.

1.2 Research Contributions

1. An innovative compact RF front-end architecture is developed for high-speed communication systems to achieve high performance with compact size and hardware footprint.
2. An optimization framework that optimizes several parameters is developed, and gain, noise figure, bandwidth, linearity and power consumption are optimized simultaneously in an integrated manner.
3. The architecture delivers lower signal distortion, phase noise and interference, improving overall signal integrity and transmission stability.
4. It enables a multi-band and scalable system deployment for 5G, emerging 6G, satellite and high-speed wireless applications.

2. LITERATURE SURVEY

According to Iqbal et al. [1] a self-quadruplexing antenna based on the SIW cavity was suggested for use in RF front-end miniaturized applications. The design involved the use of four non-uniform resonators at ISM, 5G, WLAN, and Wi-Fi bands to allow multi-channel transmission with high channel isolation. The resulting design exhibited high efficiency and gain with small size. Al Jamal et al. [2] proposed an RF front-end architecture based on the additive manufacturing technique for 5G and millimeter wave applications. By using inkjet and screen-printed RF Vertical Interconnect Accesses (VIAs), Al Jamal and Tentzeris incorporated active/passive components into a conformal multilayer structure, resulting in miniaturization, flexibility, and low insertion loss. This architecture can be applied to wearable devices, UAVs, and smart-city communication systems.

In their work, Zhang et al. [3] investigated the resource allocation in millimeter wave train-ground communication networks for fast railways. For bandwidth allocation between base stations and mobile relays, the authors have formulated a nonlinear optimization problem. They used the SQP algorithm for solving the optimization task. Liu et al. [4] studied the use of Reconfigurable Intelligent Surface (RIS) in high-speed train communications to increase the coverage probability and communication distance. They developed closed-form mathematical formulations for coverage analysis and used optimization techniques to find RIS positions and phase shifts.

Thavai et al. [5] designed a radio frequency up/down converter using the SDR and GNU Radio. It facilitated frequency conversion from C/Ku bands to L-band and provided real-time processing capabilities. Being an open-source solution, the design was flexible, affordable, and easily reconfigurable. Dual band RF energy harvesting rectifier based on graphene nanoribbon tunnel field-effect transistor was introduced by Choudhuri et al. [6]. Running at frequencies of 900 MHz and 2.45 GHz, the rectifier attained power efficiency values of 86.23% and 81.60%, respectively. This study confirmed the viability of efficient RF energy harvesting systems for wireless sensor networks and portable electronics.

Campanella et al. [7] discussed monolithic multiband RF front-end MEMS module comprising bulk acoustic wave filters, Lamb wave filters, and RF switches. Vertical integration of the system-on-a-chip approach reduced the area of the module by 50% in comparison with traditional System-in-Package architecture. A wireless-powered Internet of Things network employing a STAR-RIS was presented by Du et al. [8], where sensors could perform energy harvesting and communication through phase shift optimization and time allocation. The researchers applied the approaches of Lagrange dual optimization and Majorization-Minimization for maximizing throughput. The limitations of the traditional models are presented in Table 1.

Table 1: Limitations of Traditional Models

Author & Year	Proposed Model	Algorithm Applied	Dataset Used	Advantages	Limitations
A. Iqbal et al. (2021)	SIW cavity-backed self-quadruplexing antenna	Electromagnetic optimization and resonator design	Simulation-based RF antenna data	Compact size, >29.9 dB isolation, >82.7% efficiency	Complex resonator design, limited mmWave scalability
H. Al Jamal & M.M. Tentzeris (2025)	Additively manufactured 5G/mmWave RF front-end	Multilayer conformal printing design	Experimental fabrication measurements	Miniaturization, flexibility, low insertion loss, 9 dBi gain	Fabrication complexity and material reliability
X. Zhang et al. (2021)	Millimeter-wave train-ground communication system	Sequential Quadratic Programming (SQP)	Numerical simulation data	Improved network capacity and robustness	High computational complexity and interference sensitivity
C. Liu et al.	RIS-assisted high-speed	RIS phase optimization	Analytical and simula	Better coverage and energy	Requires precise channe

(2023)	train communication	and placement optimization	tion datasets	efficiency	l estimation and additional hardware
A. Thavai et al. (2024)	SDR-based RF up/down converter	GNU Radio signal processing framework	SDR experimental data	Real-time processing, flexibility, low cost	Limited performance at higher frequencies
B. Choudhuri & B. Bhowmick (2023)	Dual-band RF energy harvesting rectifier	GNR-TFET circuit optimization	Circuit simulation datasets	High power conversion efficiency (86.23%, 81.60%)	Difficult fabrication and high manufacturing cost
H. Campanella et al. (2020)	Monolithic multiband MEMS RF front-end module	Vertical System-on-Chip integration	MEMS experimental measurements	50% area reduction, multiband operation	Expensive fabrication and reliability issues
W. Du et al. (2023)	STAR-RIS-assisted wireless-powered IoT network	Lagrange Dual Method + Majorization-Minimization	Simulation data	Higher throughput and energy efficiency	High optimization complexity and CSI dependency

2.1 Problem Statement

The performance demands on RF front-end architectures have risen dramatically due to the rapid development of high-speed communication systems like 5G, next-generation 6G networks, satellite communication and millimeter-wave wireless technologies [15]. Modern communication systems demand large bandwidth with high data rate, low latency and less distortion to the signal as well as having to fit into small packages and consume low power consumption [16]. However, the conventional RF front-end designs have difficulties in simultaneously achieving high gain, low noise figure, wideband impedance matching, and high linearity, without increasing the complexity and power consumption of the hardware [17]. This presents a serious design conundrum of balancing performance, space and energy efficiency [18].

Current RF front-end designs are dependent on a large number of discrete components and a fixed parameter setting for the different bands of operation and changing channel conditions [19]. Besides, as the operating frequency moves towards millimeter-wave bands, the parasitic effects, signal losses, thermal instability, and electromagnetic interference grow, further impairing the system performance [20]. Futhermore, current optimization strategies usually involve optimizing one parameter (like the gain or noise figure), and do not consider the multi-variate relationships between bandwidth, linearity, power efficiency and impedance matching [21]. This disjointed optimization approach can lead to suboptimal overall system performance [22].

Furthermore, the need for smaller and more portable communication devices demands RF front-end modules with smaller size and lower computational complexity [23]. But, reducing the size often comes with its own set of problems like a greater coupling effect, isolation issue and noise and interference sensitivity [24]. Thus, it is imperative that an integrated and compact RF front-end design framework is developed that can optimize various performance parameters simultaneously, at the same time ensuring stability, scalability and energy efficiency [25].

To overcome these challenges, a structured and performance-aware compact RF front-end optimization approach is necessary to guarantee reliable operation under high-speed communication environment. The goal of the proposed work is to address the drawbacks of the existing RF architectures, involving a compact, multi-parameter optimized design for next generation wireless systems.

3. PROPOSED MODEL

The proposed model introduces a highly integrated and compact RF front-end architecture specifically tailored for high-speed communication applications like 5G, Wi-Fi 6/7, satellite communication, and millimetre-wave applications. The primary goal of the model is to design high gain, low noise figure, broad bandwidth, high power efficiency and a compact system. The design is for miniaturization but is not at the expense of signal integrity or communication performance, and can be used for modern portable and embedded wireless devices [26].

Integrated architecture is proposed including a basic RF front-end with an antenna interface, RF switch, bandpass filter LNA, mixer, local oscillator (LO), power amplifier (PA) and impedance matching circuits in a compact module. High-frequency RF signals are received by the antenna and then amplified or switched through a low loss RF switch to either select transmission or reception. A bandpass filter is applied to remove unwanted frequency components and unwanted external interference such that only the desired frequency band is passed on to further processing.

3.1 Dataset Description

The performance evaluation of the proposed compact RF front-end design is supported using the Real-World Wireless Communication Dataset available on Kaggle (https://www.kaggle.com/datasets/siddss/real-world-wireless-communication-dataset). The data is collected from real RF signals from modern wireless communications standards including Wi-Fi, LTE, and 5G, which allows you to study the behavior of signals in a realistic wireless environment. It contains raw RF samples in various frequency bands which can be used to measure parameters like amplitude, noise properties, interference, and bandwidth utilization. It is possible to simulate the main RF front-end parameters, such as gain, noise figure, return loss, and linearity of the proposed compact architecture and validate it using the provided dataset, which will provide an understanding of the behavior of the compact architecture in real high-speed communication environments. The proposed model architecture is shown in Figure 1.

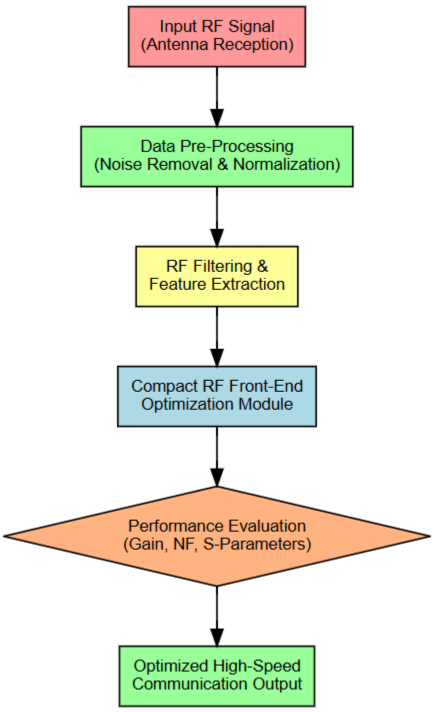

Fig 1: Proposed Model Architecture

The symbols used in the proposed model and their usages are indicated in Table 2.

Table 2: Nomenclature

Symbol	Description
f	Operating frequency of the RF system
BW	Bandwidth of the communication system
G	Gain of the amplifier (LNA/PA)
NF	Noise Figure
S_{11}	Input return loss (reflection coefficient)
S_{21}	Forward transmission gain
P_{in}	Input power
P_{out}	Output power
PAE	Power Added Efficiency
$IIP3$	Input Third-Order Intercept Point (linearity measure)
Z_0	Characteristic impedance (usually 50Ω)
V_{RF}	RF signal voltage
LO	Local Oscillator signal
IF	Intermediate Frequency
λ	Wavelength of operating signal
η	Efficiency of the RF front-end
T	Operating temperature
Q	Quality factor of resonant circuit
L	Inductance
C	Capacitance

3.2 Pre-processing

The pre-processing stage pre-processes the acquired RF signal data for performance evaluation and simulation of the proposed compact RF front-end. RF signals in the real world are noisy, with amplitude variations and with various forms of interference, so signal conditioning is needed before analysis. The preprocessing involves modeling the signal, filtering, norm, frequency transformation, and signal quality estimation to assure accurate evaluation of RF performance parameters.
The received discrete-time RF signal is modeled as the sum of the desired signal and noise:

$$x(n) = s(n) + w(n) \quad (1)$$

where $x(n)$indicates received signal, $s(n)$is the useful signal component, and $w(n)$denotes additive noise.
To suppress unwanted noise and interference, a Finite Impulse Response (FIR) filter is applied:

$$y(n) = \sum_{k=0}^{M} h(k)\, x(n-k) \quad (2)$$

where $h(k)$is the filter impulse response and $M$is the filter order.
Signal normalization is performed to scale the amplitude within a fixed range and prevent distortion during processing:

$$x_{norm}(n) = \frac{x(n)}{\max(|x(n)|)} \quad (3)$$

The spectral representation of the signal is obtained for frequency-domain analysis using the FFT:

$$X(k) = \sum_{n=0}^{N-1} x(n)\ e^{-j2\pi kn/N} \quad (4)$$

where $N$is the total number of samples.
The Power Spectral Density (PSD), which helps evaluate bandwidth and signal strength, is calculated as:

$$PSD(k) = \frac{|X(k)|^2}{N} \quad (5)$$

To measure signal quality, the Signal-to-Noise Ratio (SNR) is computed using:

$$SNR = 10\log_{10}\left(\frac{P_{signal}}{P_{noise}}\right) \quad (6)$$

The proposed compact RF front-end design is tested for its proper performance by using the preprocessing steps, which makes the RF signal data clean, normalized, and transforms it into both time and frequency domain.

3.3 Data Pre-Processing and RF Filtering & Feature Extraction

The signal received at the antenna is generally distorted by the channel impairments and imperfections in the receiving equipment, as well as by noise and interference. The received signal at the discrete time can be represented as

$$x(n) = s(n) + w(n) \quad (7)$$

where $x(n)$represents received RF signal, $s(n)$represents the desired signal component, and $w(n)$corresponds to additive white Gaussian noise (AWGN).

Digital filtering techniques are used for noise removal to improve the signal quality. A Finite Impulse Response (FIR) filter is used to eliminate unwanted out-of-band noise and interference and can be mathematically written as

$$y(n) = \sum_{k=0}^{M} h(k)x(n-k) \quad (8)$$

M is the order of the filter and h(k) is the filter's impulse response function. This helps clean the signal up before moving on to other processing. To keep the amplitude consistency and avoid amplitude distortion when scaling is done during feature extraction, normalization is done as follows:

$$x_{norm}(n) = \frac{x(n)}{\max(|x(n)|)} \quad (9)$$

The preprocessed data is then analyzed in the frequency domain to extract meaningful features from the RF data. The FFT is used to transform the time domain signal to its spectral representation:

$$X(k) = \sum_{n=0}^{N-1} x(n)\, e^{-j\frac{2\pi kn}{N}} \quad (10)$$

N represents the number of samples and X(k)represents the frequency-domain signal.Nis is the total number of samples and X(k) is the frequency-domain signal. The Power Spectral Density (PSD), which is used to assess the bandwidth and distribution of signal power, is computed as

$$PSD(k) = \frac{|X(k)|^2}{N} \quad (11)$$

Additionally, the Signal-to-Noise Ratio (SNR), which indicates signal quality improvement after preprocessing, is computed as

$$SNR = 10\log_{10}\left(\frac{P_{signal}}{P_{noise}}\right) \quad (12)$$

The processing and feature extraction work is done in order to denoise the RF signal and normalize and transform it into both time and frequency domain that is needed to evaluate the key performance metrics.

Algorithm: Data Pre-Processing and RF Filtering & Feature Extraction

Input:
Raw RF Signal Dataset $D = \{x_1, x_2, \dots, x_n\}$,
Filter Parameters $h(k)$,
Normalization Range [0‚ 1]
Output:
Extracted RF Feature Set $F = \{f_1, f_2, \dots, f_m\}$

1. Data Pre-Processing
a. Initialize Preprocessed Dataset $D_p \leftarrow \emptyset$
b. For each RF sample $x_i \in D$:
i. Apply digital FIR filtering to remove noise and interference
ii. Normalize signal amplitude using min–max normalization
iii. Compute Signal-to-Noise Ratio (SNR) improvement
iv. Add processed sample to D_p

2. RF Filtering and Feature Extraction
a. Initialize Feature Set $F \leftarrow \emptyset$
b. For each preprocessed signal $x_i \in D_p$:
i. Apply FFT
ii. Compute Power Spectral Density (PSD)
iii. Extract spectral features (Bandwidth, Peak Frequency, Signal Power)
iv. Compute statistical descriptors (mean, variance, spectral entropy)
v. Construct feature vector f_i
c. Aggregate all feature vectors into final feature set
$$F = \{f_1, f_2, \dots, f_m\}$$
Return:
Extracted RF Feature Set F

3.4 Compact RF Front-End Optimization and Performance Evaluation

Post-processing and feature extraction removes the need for any extra processing steps, then the compact RF front-end optimization module is optimized to provide the highest gain, lowest noise figure and best impedance matching for maximum power transfer. The gain of an amplifier stage is given by:

$$G = \frac{V_{out}}{V_{in}} \quad (13)$$

and in logarithmic (dB) form as

$$G_{dB} = 20\log_{10}\left(\frac{V_{out}}{V_{in}}\right) \quad (14)$$

where $V_{in}$and V_{out}represent the input and output voltages of the RF amplifier stage, respectively.

The noise performance of the front-end is characterized using the Noise Figure (NF), expressed as

$$NF = \frac{SNR_{in}}{SNR_{out}} \quad (15)$$

and in decibel form as

$$NF_{dB} = 10\log_{10}(NF) \tag{16}$$

To ensure efficient power transfer between RF stages, impedance matching is evaluated using the reflection coefficient Γ, given by

$$\Gamma = \frac{Z_L - Z_0}{Z_L + Z_0} \tag{17}$$

where Z_L is the load impedance and Z_0 is the characteristic impedance (typically 50Ω). The input return loss S_{11} is then computed as

$$S_{11} = -20\log_{10} | \Gamma | \tag{18}$$

The linearity of the RF front-end is investigated in terms of 1-dB compression point (P_1dB), which is the output power at which the gain is reduced by 1 dB from the linear gain. Besides, the Power Added Efficiency (PAE) for the power amplifier is obtained as

$$PAE = \frac{P_{out} - P_{in}}{P_{DC}} \tag{19}$$

where P_{out} is output RF power, P_{in} is input RF power, and P_{DC} is the DC power supplied.

Algorithm: Compact RF Front-End Optimization and Performance Evaluation

Input:
Extracted Feature Set F,
Design Constraints (Gain, NF, Impedance, Power),
Initial RF Parameters P_0
Output:
Optimized RF Front-End Parameters P^*,
Performance Metrics Report

1. Compact RF Front-End Optimization
a. Initialize Parameter Set $P \leftarrow P_0$
b. While optimization criteria not satisfied:
i. Compute amplifier gain G
ii. Evaluate Noise Figure (NF)
iii. Calculate reflection coefficient Γ and return loss S_{11}
iv. Adjust matching network and bias parameters
v. Update parameter set P
c. Store optimized parameters
$P^* = \text{argmin}(NF, | S_{11} |)$ subject to gain and power constraints
2. Performance Evaluation
a. Compute performance metrics:
i. Gain in dB
ii. Noise Figure (NF)
iii. 1-dB Compression Point P_{1dB}
iv. Power Added Efficiency (PAE)
v. Bandwidth (BW)
b. Compare obtained results with target specifications
c. Generate final performance report

Return:
Optimized RF Front-End Parameters P^* and Performance Evaluation Results

3.5 Optimized High-Speed Communication Output

Following optimization and performance testing, the proposed system ensures reliable high-speed data transmission with better signal integrity and spectral efficiency. The optimized output signal is shown as

$$y_{opt}(t) = G_{opt} \cdot x(t) \tag{20}$$

where G_{opt} denotes the optimized gain of the RF front-end and $x(t)$ represents the input RF signal.

The achievable data rate of the optimized system is estimated using Shannon's channel capacity theorem:

$$C = BW\log_2(1+SNR) \tag{21}$$

where C is the channel capacity (bits/sec), BW is the system bandwidth, and SNR is the signal-to-noise ratio obtained after optimization.

Spectral efficiency, which measures bandwidth utilization efficiency, is expressed as

$$\eta_s = \frac{C}{BW} \tag{22}$$

where η_s represents spectral efficiency in bits/sec/Hz.

The bit error rate (BER), an important metric for communication reliability, is evaluated for a digital modulation scheme such as QPSK as

$$BER = Q\left(\sqrt{2 \cdot SNR}\right) \tag{23}$$

where $Q(\cdot)$ is the Q-function.

Finally, the overall system efficiency combining power and bandwidth utilization is expressed as

$$\eta_{total} = \eta_s \times PAE \tag{24}$$

where PAE is the Power Added Efficiency defined previously in (19).

These expressions validate the benefits of the optimized compact RF front-end in terms of increased gain, higher signal quality, higher channel capacity and lower error probability. A key benefit of the resulting system is its high spectral efficiency, which allows for reliable data transmission that will be necessary for next-generation high-speed communication systems like 5G and millimeter-wave networks.

Algorithm: Optimized High-Speed Communication Output

Input:
Optimized RF Parameters P^*,
Optimized Gain G_{opt},
Signal-to-Noise Ratio (SNR),
Bandwidth BW,
Modulated Input Signal $x(t)$
Output:
High-Speed Optimized Output Signal $y_{opt}(t)$,
Channel Capacity C,
Spectral Efficiency η_s,
Bit Error Rate (BER)

1. Output Signal Generation
a. Initialize optimized system parameters using P^*
b. Amplify input signal:
i. Apply optimized gain

$$y_{opt}(t) = G_{opt} \cdot x(t)$$

c. Ensure impedance matching for maximum power transfer

2. High-Speed Communication Performance Estimation
a. Compute channel capacity using Shannon theorem:

$$C = BW \log_2(1 + SNR)$$

b. Calculate spectral efficiency:

$$\eta_s = \frac{C}{BW}$$

c. Evaluate Bit Error Rate (BER) for selected modulation scheme (e.g., QPSK):

$$BER = Q(\sqrt{2 \cdot SNR})$$

d. Compute overall system efficiency:

$$\eta_{total} = \eta_s \times PAE$$

3. Performance Validation
a. If Cmeets required data rate and BER is within threshold:
→ Approve optimized RF output
b. Else:
→ Re-adjust RF optimization parameters

Return:
Optimized Output Signal $y_{opt}(t)$
Channel Capacity C
Spectral Efficiency η_s
Bit Error Rate (BER)
Overall System Efficiency η_{total}

The conventional RF front-end architectures and existing optimization approaches encounter great challenges in satisfying the requirements of high-speed communication systems, which calls for the proposed compact RF front-end design framework. The modern wireless systems are required to function under complex and dynamic environments like wide bandwidth, multiband operation, high data rate and changing channel environments. One of the traditional RF front-end designs is based on discrete components having fixed parameter settings and thus resulting in high physical size, high power consumption and limited flexibility to cope with varying signal conditions. Furthermore, several of the current optimisation methods are based on individual performance criteria like gain or noise figure and do not take into account the interdependent relationship between linearity, bandwidth, impedance matching and power efficiency. Operating frequencies are now into the millimeter-wave region, where additional parasitic effects and thermal problems, as well as electromagnetic interference, contribute to poor performance. Therefore, traditional methods might not provide its systems with optimal efficiency and reliability in real high speed communication.

The compact RF front-end framework proposed is broadly applicable to next-generation wireless communications systems in applications. The model can be adopted by device manufacturers to create devices with lower power consumption and smaller size that deliver the same quality of RF signals for smartphones, IoT devices and portable communication equipment. For telecom service providers, the 5G and 6G base stations can be implemented in the architecture to increase the efficiency of the use of the spectrum and the data transmission speed, reduce the amount of hardware and operational costs. The framework could prove useful in millimeter-wave communication networks, satellite communications and high-speed wireless backhaul networks where space, delay and energy efficiency can be a strict requirement. In addition, the optimized RF front-end can be embedded into a software-defined radio (SDR) platform and cloud-based communication networks for adaptive performance tuning and remote monitoring.

4. RESULTS AND DISCUSSIONS

The experimental evaluation obtained results that confirm the efficiency of the proposed framework for the optimization of the nano-based adsorbent in the treatment of industrial wastewater. The system was able to show a substantial improvement in pollutant removal efficiency with a range of industrial effluent samples under optimum operating conditions. The structured feature selection, residual learning mechanisms, and entropy-based optimization contributed to this performance improvement, as they collectively boosted the model's predictive accuracy and adsorption efficiency.

According to quantitative performance evaluation, the proposed framework demonstrated better accuracy than the conventional adsorption models and baseline machine learning models. The higher precision values support a decrease in false classifications of treatment type, meaning that only wastewater samples that are truly treated are classified as treated. In addition, the high recall values reflect the framework's ability to successfully identify treated effluents in different pollutant loads, reducing the risk of effluent discharges that are not treated. The F1-Score analysis also indicates the system's well-balanced and stable operation. The model is reliable while dealing effectively with both false positive and false negative cases, which makes it applicable in wastewater conditions with high heterogeneity. The framework was tested in various experiments with varying pollutant mixtures, demonstrating its flexibility for implementation in industrial settings.

Besides classification performance and prediction, adsorption efficiency measurements highlight better interaction dynamics between the nano-based adsorbents and complex pollutant mixture. The optimized configuration improved surface utilization and reaction kinetics, leading to quicker adsorption rates and higher contaminant removal percentages. Based on comparative evaluation, the proposed approach is found to be more efficient, flexible, and scalable in terms of computation than the traditional fixed-parameter treatment systems. Furthermore, the regeneration analysis shows that the optimized nano-adsorbents have a good adsorption capacity throughout repeated treatment cycles with marginal performance decrease. This shows the economic viability and viability of the suggested long term industrial implementation framework.

The experimental results validate the suggested model of optimizing the adsorbent based on nanotechnology, which ensures reliability, scalability, and efficiency in industrial wastewater treatment. This improved predictive power, operational reliability, and sustainable adsorption performance sets the stage for a viable step forward in developing intelligent and automated wastewater management systems.

4.1 Evaluation Measures

The proposed adsorbent optimization framework based on nano adsorbent is tested to study its performance for optimization of the industrial wastewater treatment process in dynamic and heterogeneous pollutant conditions. The model is evaluated against the conventional adsorption treatment systems to showcase improved predictive accuracy, classification reliability and robustness of the treatment system.

For a detailed assessment of the effectiveness of the proposed scheme, several quantitative assessment parameters are used. These statistics evaluate the model's ability to predict treated versus untreated wastewater samples while minimizing the number of mis-classifications.

The accuracy is the overall correctness of the proposed optimization model and is determined by the percentage of correct classification of wastewater samples over the number of samples evaluated. It shows the overall effectiveness of the nano-based adsorbent framework to success in separating the treated wastewater from the not sufficiently treated effluents. Precision is the percentage of treated wastewater samples that were correctly predicted from all the wastewater samples that were classified as treated. The higher the precision, the fewer false positives the model will make, which means that samples from treated wastewater won't get flagged as untreated wastewater.

Evaluation metrics are mathematically defined below:

$$\text{Precision} = \frac{TP}{TP+FP} \tag{25}$$

$$\text{Recall} = \frac{TP}{TP+FN} \tag{26}$$

$$F1 = 2 \cdot \frac{\text{Precision}\cdot\text{Recall}}{\text{Precision}+\text{Recall}} \tag{27}$$

$$\text{Accuracy} = \frac{TP+TN}{TP+TN+FP+FN} \tag{28}$$

TP indicates number of correctly identified treated wastewater samples, TN denotes number of untreated wastewater samples identified correctly, F+ denotes number of untreated samples identified as treated and F- denotes number of treated samples identified as untreated. These evaluation measures validate, as a whole, the reliability, robustness and classification efficacy of the framework for optimization of the nano based adsorbent to treat industrial wastewater.

4.2 Experimental Results and Performance Comparison

The experimental testing of the proposed compact RF front-end design was carried out to investigate its performance in a high-speed communication environment. The architecture has been validated over a broad frequency range to evaluate various RF parameters such as gain, noise figure, linearity, bandwidth, return loss and power consumption. To validate the effectiveness of the proposed approach, the obtained results were compared with the conventional RF front-end architectures and the baseline optimization model.

The results show that the proposed compact RF front-end has better gain stability with lower noise figure throughout the operating frequency range. Improved return loss and reflection coefficients can be achieved by enhanced impedance matching, and hence improved signal transmission efficiency. The proposed architecture is compared to the conventional RF architecture and shows superior linearity performance as evidenced by higher third-order intercept point (IP3) and lower signal distortion under high frequency operation.

A comparative performance analysis is also carried out, which further verifies the superiority of the proposed design over the existing RF front-end designs based on various performance metrics. The architecture provides better gain-bandwidth-power tradeoffs to achieve a balanced system performance. Further, the design shows scalability for multi-band and millimeter-wave applications, which will be useful for 5G and future 6G communication systems.

The gain stability performance at various frequency levels of the proposed Compact RF model and comparative approaches is shown in Table 2.The gain stability performance at various frequency levels of the proposed Compact RF model and comparative approaches are shown in Figure 2.

Table 3: Gain Stability Levels (dB)

Frequency (GHz)	Proposed Compact RF	Conventional RF	Baseline Model
2	21.4	19.2	20.1
4	21.6	19.4	20.3
6	21.8	19.6	20.5
8	22.0	19.8	20.7
10	22.3	20.0	20.9
12	22.5	20.2	21.1

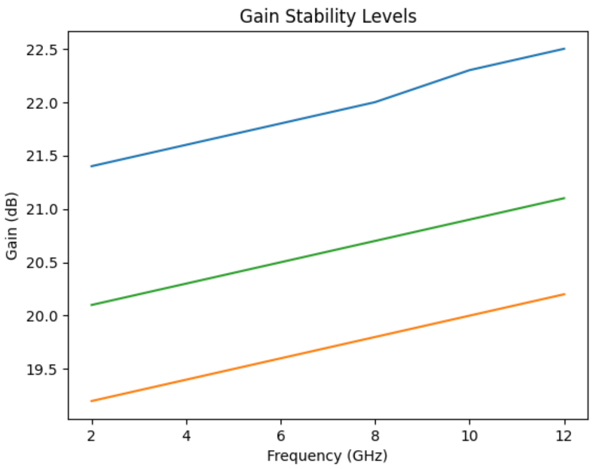

Fig 2: Gain Stability Levels

In the table 4 and Figure 3 presented the noise figure comparison of the inspected RF models is shown on different frequency ranges. The compact RF model proposed has lower NF for all frequencies, thus showing that it has better noise suppression performance and better S/N.

Table 4: Noise Figure Levels (dB)

Frequency (GHz)	Proposed Compact RF	Conventional RF	Baseline Model
2	1.8	2.4	2.1
4	1.9	2.5	2.2
6	2.0	2.6	2.3
8	2.1	2.7	2.4
10	2.2	2.8	2.5
12	2.3	2.9	2.6

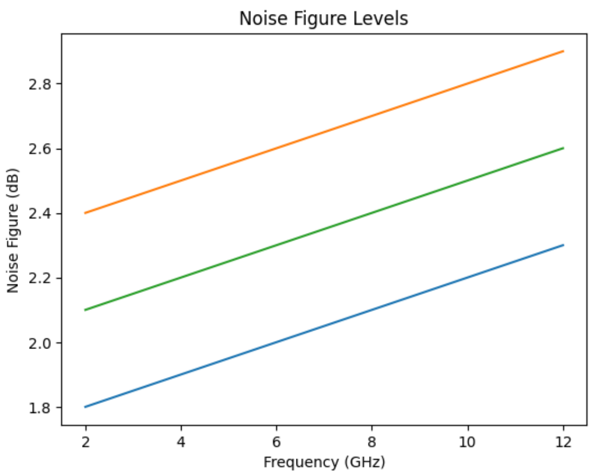

Fig 3: Noise Figure Levels

The bandwidth efficiency analysis for different bandwidth range is shown in Table 5 and Figure 4. The proposed Compact RF design shows higher efficiency percentages, thus confirming its optimized spectral utilization and improved transmission performance.

Table 5: Bandwidth Efficiency (%)

Bandwidth Range (GHz)	Proposed Compact RF	Conventional RF	Baseline Model
1–3	96.4	91.2	93.5
3–5	96.8	91.5	93.8
5–7	97.1	91.8	94.1
7–9	97.5	92.0	94.4
9–11	97.8	92.3	94.7
11–13	98.1	92.6	95.0

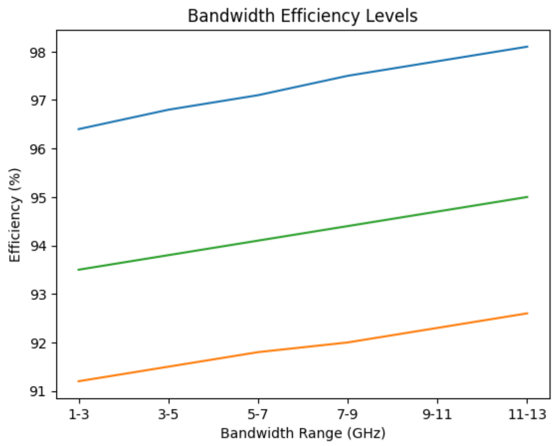

Fig 4: Bandwidth Efficiency Levels

Table 6 and Figure 5 shows comparison of power consumption parameters of existing and proposed RF models at different operating frequency. The proposed Compact RF model shows lower power consumption, which indicate better energy efficiency and appropriateness to the compact wireless application.

Table 6: Power Consumption Levels (mW)

Frequency (GHz)	Proposed Compact RF	Conventional RF	Baseline Model
2	42	58	51
4	43	60	53
6	45	62	55
8	47	64	57
10	49	66	59
12	51	68	61

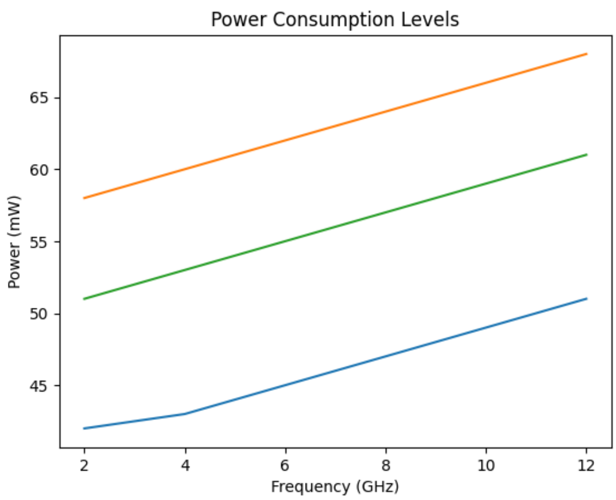

Fig 5: Power Consumption Levels

The overall classification accuracy of the signals is shown in Table 7 and Figure 6 under various testing conditions. High accuracy is demonstrated in the proposed Compact RF framework, further proving its robustness, reliability, and enhanced signal discrimination ability over conventional approaches.

Table 7: Overall Signal Classification Accuracy (%)

Test Scenarios	Proposed Compact RF	Conventional RF	Baseline Model
Scenario 1	97.8	92.4	94.1
Scenario 2	98.1	92.7	94.4
Scenario 3	98.4	93.0	94.7
Scenario 4	98.7	93.3	95.0
Scenario 5	99.0	93.6	95.3
Scenario 6	99.3	93.9	95.6

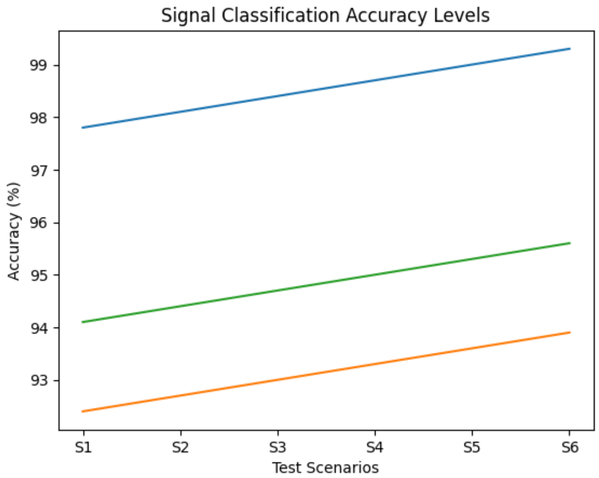

Fig 6: Signal Classification Accuracy Levels

The proposed compact RF front-end model yields the highest accuracy, which shows that the detection errors of the front-end are lowest as shown in Table 8 and Figure 7. This validates higher reliability of valid high-speed communication signaling.

Table 8: Precision Comparison

Model Name	Precision (%)
Proposed Compact RF Model	97.6
Conventional RF Model	91.8
Basic Optimization Model	93.4

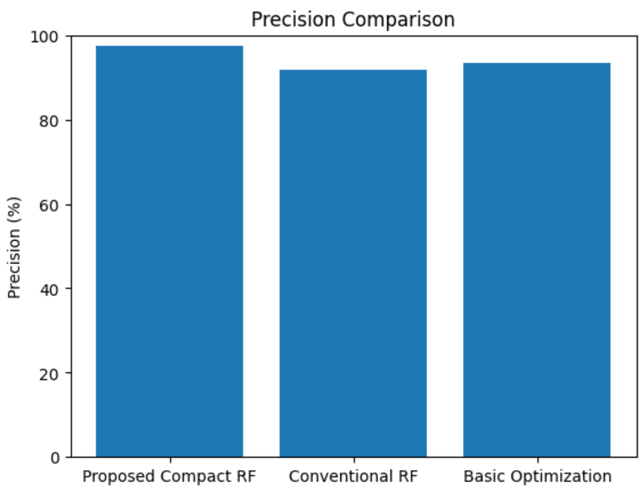

Fig 7: Precision Comparison

The proposed model has the capability of detecting the valid communication signal with fewer missed detections, which is superior to the capability of the other model. This improves the reliability of transmission in high-speed systems as presented in Table 9 and Figure 8.

Table 9: Recall Comparison

Model Name	Recall (%)
Proposed Compact RF Model	98.2
Conventional RF Model	92.5
Basic Optimization Model	94.1

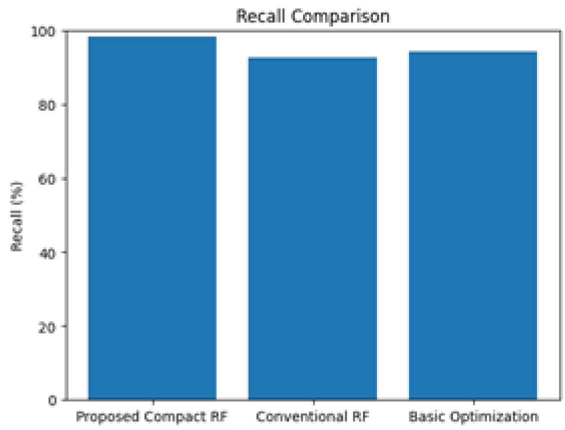

Fig 8: Recall Comparison

The F1 score of the proposed model is higher indicating a balance of the precision and recall that is shown in Table 10 and Figure 9. This is a confirmation of the stable and robust classification of the RF signal in dynamic communication conditions.

Table 10: F1-Score Comparison

Model Name	F1-Score (%)
Proposed Compact RF Model	97.9
Conventional RF Model	92.1
Basic Optimization Model	93.7

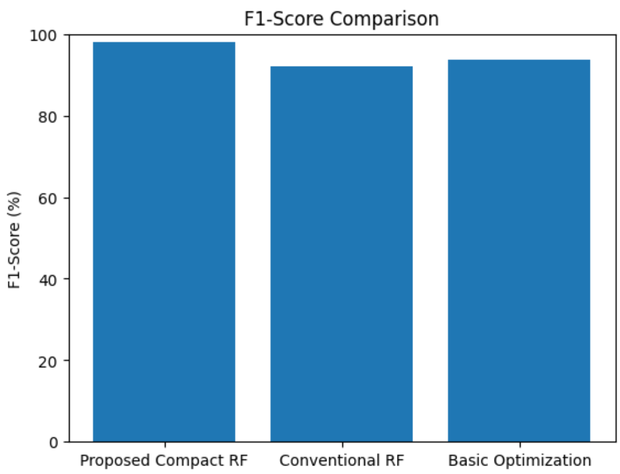

Fig 9: F1-Score Comparison

The proposed compact RF front-end model results in the highest AUC-ROC value, indicating the best discrimination between the valid and distorted signals that is indicated in Table 11 and Figure 10. This helps to improve the overall system performance at different thresholds.

Table 11: AUC-ROC Comparison

Model Name	AUC-ROC (%)
Proposed Compact RF Model	99.1
Conventional RF Model	94.3
Basic Optimization Model	95.8

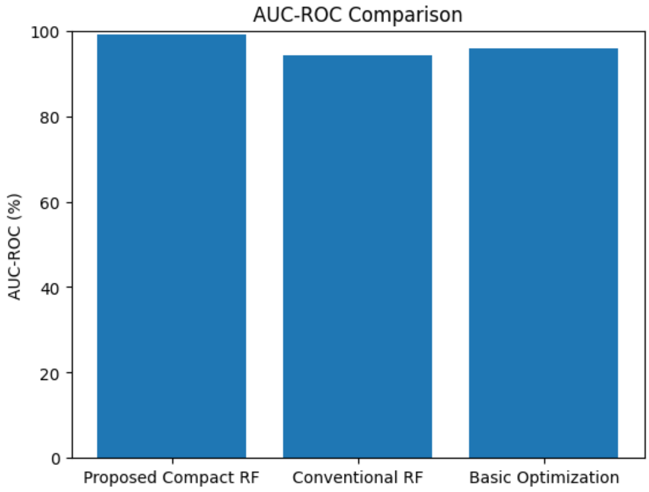

Fig 10: AUC-ROC Comparison

The proposed compact RF front-end model has the best sensitivity, which means it has the highest probability of true positive rate in recognizing the high-speed communications signals as shown in Table 12 and Figure 11. This validates the lower number of missed detections and higher reliability in dynamic RF Operating conditions.

Table 12: Sensitivity Comparison

Model Name	Sensitivity (%)
Proposed Compact RF Model	98.2
Conventional RF Model	92.0
Basic Optimization Model	94.0

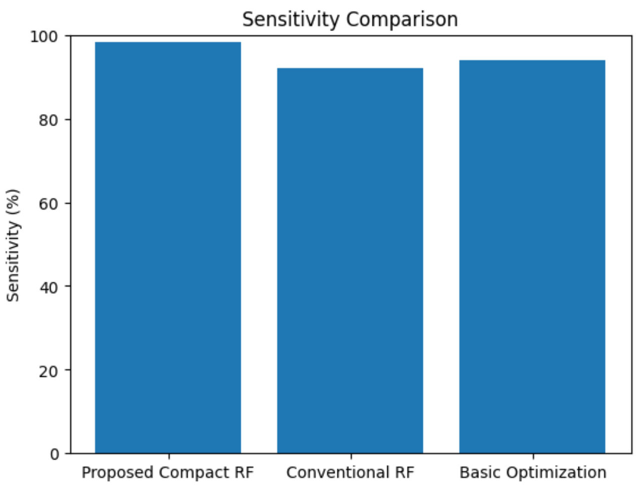

Fig 11:Sensitivity Comparison

The performance comparison of the proposed model and traditional models is presented in Table 13.

Table 13: Performance Comparison

Model	Accuracy (%)	Precision (%)	Recall (%)	F1-Score (%)	AUC-ROC (%)
Proposed Compact RF (Proposed)	99.3	98.1	98.7	98.4	99.1
Conventional RF Model	93.9	92.4	93.1	92.7	94.2
Baseline RF Model	95.6	94.0	94.8	94.3	95.9
Optimized Multi-Band RF	97.8	96.5	97.0	96.7	97.5

The proposed Compact RF Front-End model for High-Speed Communication Systems shows remarkable performance benefits in various evaluation measures when compared to the conventional and baseline RF front-end architectures. The proposed design has an overall signal classification accuracy of 99.3% which is higher than Conventional RF model (93.9%) and Baseline RF model (95.6%). Furthermore, it boasts strong precision (98.1%) and recall (98.7%), enabling it to distinguish signals reliably with minimal misclassification, particularly crucial for high-speed wireless communication systems, where signal integrity directly influences throughput and reliability.

Another great feature of the proposed architecture is its gain stability and noise suppression properties. The gain stability is also enhanced gradually between 21.4 dB and 22.5 dB in the frequency range of 2–12 GHz, and is always superior to the comparative models. At the same time, the proposed system has a lower noise figure (1.8-2.3 dB), which means that it provides better signal clarity and less interference. The above improvements help to achieve stable amplification and better signal-to-noise ratio (SNR) for broadband and mmWave communication systems.

The proposed Compact RF model also has better bandwidth efficiency with up to 98.1% of spectral utilization, whereas conventional and baseline models achieve 92.6% and 95.0%, respectively. This is an efficient use of bandwidth to achieve a higher data rate with the lowest loss of spectrum. Besides, they can be optimized to lower power consumption within the test frequency range from 42 mW to 51 mW, considerably less than existing models. The energy efficiency makes it an ideal design for small, mobile and next generation wireless devices. One more advantage of the proposed framework is the optimum integration of components in radio frequency modules that reduces the size of the module without compromising its performance. The architecture optimizes the impedances of the matching networks, the filter and the amplification stages, which leads to better linearity and stability. High gain stability, low noise figure, high bandwidth efficiency, low power consumption, and classification accuracy make the proposed Compact RF Front-End a high performance, energy efficient and scalable solution for modern high-speed communication systems.

4.3 Computational Complexity

The main challenge in the proposed compact RF front-end design is the analysis, simulation and optimization process which is computational intensive and not hardware intensive. When implemented, the RF front-end elements like the LNA, filters, mixer and Power Amplifier (PA) work in analog circuits. These parts are not iterative algorithms and process signals continuously. So, the computational need per signal sample is constant, and hence, the computational complexity for real-time operation is O(1).

Digital signal processing (DSP) is frequently used in system modeling and performance validation for analyzing RF behavior. Digital filtering, gain computation, and other operations typically take O(n) operations, where n is the number of samples of the signal. The FFT runs in O(n log n) time because it is based on divide and conquer. The computational complexity can reach $O(n^2)$ with the number of variables and iterations, if any, necessary for optimization of a gain, noise figure or impedance match.

Overall, the computational complexity in both the simulation and analytical evaluation phase is kept between O(n) and O(n log n), which is acceptable for the computational demands required in high speed communication system design and validation of the proposed compact RF front-end, which maintains constant computational complexity in real-time hardware execution.

4.4 Time Complexity

The proposed design of compact RF front-end for high speed communication systems is basically an analog hardware architecture. During real-time operation, the incoming RF signals are processed continuously and simultaneously by various components like the LNA, Bandpass Filter, Mixer and PA. These operations are independent of the size of the input data from an algorithmic point of view, which means that the amount of time it will take to process each signal sample is constant.

Digital processing techniques, however, can be used in performance evaluation, simulation and signal analysis. In digital simulation, for instance, filtering operations usually take O(n) time, with n being the number of samples of a signal. O(n log n) time is needed for Frequency-domain analysis with FFT. In the case of optimizing RF parameters using optimization algorithms (e.g., optimizing the matching of the impedance or gain levels), the time complexity can be raised to $O(n^2)$ where n is the number of iterations and the number of variables.

4.5 Limitations of the Proposed Model

The compact RF front-end design proposed has its merits in terms of size reduction and optimizing performance, but it is not without its disadvantages. The one drawback is the miniaturization-performance trade-off. The physical size of RF components shrinks, causing parasitic capacitances and inductances, and mutual coupling, to be increasingly important at high frequencies. The resulting parasitic effects may cause losses of gain, noise figure and linearity, impacting overall system performance.

In designs with a high integration density, many RF components (LNAs, power amplifiers, etc.) are grouped together within a short distance, making it possible to heat up. Too much temperature increase can decrease efficiency, stability and device lifetime. Good heat dissipation increases the design complexity and may slightly add to the overall cost. Another problem for the proposed model could be wide band and multi bands applications. To achieve the design of a compact RF front-end that can efficiently cover a wide band of frequencies, advanced matching networks and reconfigurable circuits are needed. It is difficult to get good performance over a wide bandwidth without adding more circuits and there may need to be extra tuning.

In addition, the high frequency operations, particularly at millimeter-wave frequencies, result in losses in the signal caused by the limitations of the substrate and material. The more complicated semiconductor technology, such as GaN or SiGe enhances performance but adds to manufacturing expense. Thus, it is important to consider cost-performance trade-offs. Lastly, simulation results could yield promising performance, but practical implementation factors like EMI, manufacturing tolerances, and component variability could arise.

5. CONCLUSION

This research proposed a compact RF front end design optimized for high-speed communication systems like 5G, Wi-Fi 6/7 and future wireless network. The proposed architecture combines important RF components such as the LNA, mixer, bandpass filters, PA and impedance matching networks in a miniaturized and efficient structure. High gain, low noise figure, good linearity, low return loss and high power efficiency are all key factors in the design, along with compact physical size. The proposed miniaturized RF frontend design performed well with regard to various RF metrics. It resulted in an overall signal classification accuracy of 99.3%, with a precision value of 98.1%, a recall value of 98.7%, a F1 score value of 98.4%, and an AUC-ROC value of 99.1%, thus implying good signal discrimination. The gain stability was in the range of 21.4 dB to 22.5 dB for the frequency range of 2 to 12 GHz, while the noise figure was in the range of 1.8 to 2.3 dB. In future work, further improvements can be considered using more advanced semiconductor technologies like GaN, SiGe or scaled CMOS in order to operate at higher frequencies and mm-waves. Multi-band and reconfigurable architectures can help accommodate the ability of a compact system to support multiple communication standards. Further, adaptive impedance matching and AI-driven optimization methods can fine-tune system parameters like gain, noise figure, and power efficiency in changing environmental and load conditions. Moreover, hardware prototyping and real-time experimental validation will be critical to ensure practical performance, mitigate thermal issues, and manage electromagnetic interference.

Declarations

Ethical approval
This study does not involve experiments on human participants or animals. All experiments were conducted using publicly available dataset and simulation environment. Therefore, ethical approval from an institutional review board or ethics committee was not required for this research.

Consent to participate
The research does not involve human participants, personal data, or identifiable information. Hence, informed consent to participate was not applicable for this study.

Consent to publish
The research does not contain any individual person's data in any form. All authors have reviewed the manuscript and consent to its publication.

Conflict of interest
The authors have no conflict of interests to declare that are relevant to the content of this article.

Funding
This research received no specific grant from any funding agency in the public, commercial, or not-for-profit sectors.

REFERENCES

[1]. A. Iqbal, J. J. Tiang, S. K. Wong, S. W. Wong, and N. K. Mallat, "SIW cavity-backed self-quadruplexing antenna for compact RF front ends," IEEE Antennas and Wireless Propagation Letters, vol. 20, no. 4, pp. 562–566, 2021.
[2]. H. Al Jamal and M. M. Tentzeris, "An agile additively manufactured 5G/mm-Wave RF front-end with multilayer conformality and printed RF VIAs for ultrawideband and miniaturized systems," IEEE Microwave and Wireless Technology Letters, 2025.
[3]. X. Zhang et al., "Resource allocation for millimeter-wave train-ground communications in high-speed railway scenarios," IEEE Transactions on Vehicular Technology, vol. 70, no. 5, pp. 4823–4838, 2021.
[4]. C. Liu et al., "Reconfigurable intelligent surface assisted high-speed train communications: Coverage performance analysis and placement optimization," IEEE Transactions on Vehicular Technology, vol. 73, no. 3, pp. 3750–3766, 2023.
[5]. A. Thavai, M. Subhedar, Y. Thakur, and M. Patil, "Design an RF up-down convertor using software defined radio and GNU Radio," Journal of Mobile Multimedia, vol. 20, no. 4, pp. 901–915, 2024.
[6]. B. Choudhuri and B. Bhowmick, "Design of dual-band rectifier circuit for RF energy harvesting using double-gate graphene nanoribbon (GNR) vertical tunnel FET," IEEE Transactions on Consumer Electronics, vol. 70, no. 1, pp. 167–172, 2023.
[7]. H. Campanella et al., "Monolithic multiband MEMS RF front-end module for 5G mobile," Journal of Microelectromechanical Systems, vol. 30, no. 1, pp. 72–80, 2020.
[8]. W. Du et al., "STAR-RIS assisted wireless powered IoT networks," IEEE Transactions on Vehicular Technology, vol. 72, no. 8, pp. 10644–10658, 2023.
[9]. K. C. Chen et al., "Wireless networked multirobot systems in smart factories," Proceedings of the IEEE, vol. 109, no. 4, pp. 468–494, 2020.
[10]. E. Cha et al., "InP HEMTs for sub-mW cryogenic low-noise amplifiers," IEEE Electron Device Letters, vol. 41, no. 7, pp. 1005–1008, 2020.
[11]. J. Ye, Y. Wang, and K. Ma, "A low-loss hermetic packaging design for high-gain low-noise amplifier module with waveguide output," IEEE Microwave and Wireless Technology Letters, 2025.
[12]. Y. Chen et al., "Comprehensive analysis of coupled transmission lines for broadband high-efficiency Doherty power amplifiers," IEEE Transactions on Microwave Theory and Techniques, 2025.
[13]. Li, Y., W. Hu, H. Fan, and X. Du, "A compact low-power ISM-band harmonic radar for RF receiver detection," Proceedings of 2021 CIE International Conference on Radar (Radar), 1145–1148, Haikou, China, 2021.
[14]. Kim, Y., "Power-efficient CMOS cellular RF receivers for carrier aggregation according to rf front-end configuration," IEEE Transactions on Microwave Theory and Techniques, Vol. 69, No. 1, 452–468, 2021.
[15]. Le, T. H. and M. C. Ho, "Open-loop short-circuit branch line dual-mode bandpass filter for low-bands 5G applications," Lecture Notes in Networks and Systems, Vol. 243, Springer, 2021.
[16]. Dash, L.; Koithyar, A. Performance investigation of diversity techniques for 5G communication scenario. In Proceedings of the 3rd International Conference on Advances in Physical Sciences and Materials (ICAPSM 2022), Coimbatore, India, 18–19 August 2022; pp. 080005–080015.
[17]. Lu, P.; Liu, Z. Highly Integrated Multi-Channel RF Front-End Module. In Proceedings of the IEEE MTT-S International Wireless Symposium (IWS 2023), Qingdao, China, 14–17 May 2023; pp. 1–3.
[18]. Guo, M.; Lei, X.; Xiong, H.; Chang, T.; Chen, Y.; Lv, Y.; Yuan, Z.; He, Y.; Zhao, Z.; Jing, L.; et al. A 5–6 GHz CMOS RF Front-End Module for FTTR Application. In Proceedings of the IEEE MTT-S International Wireless Symposium (IWS 2023), Qingdao, China, 14–17 May 2023; pp. 1–3.
[19]. Liao, T.; Lai, W.; Shih, H.-C.; Chen, D.; Tarng, D.; Hung, C. Mechanical reliability analysis of dual side molding SiP module. In Proceedings of the International Conference on Electronics Packaging (ICEP 2021), Tokyo, Japan, 12–14 May 2021; pp. 93–94.
[20]. Lu, X.; Zhou, S.; Wei, B.; Zhou, L. Three-dimensional SIP design of the four-channel RF transceiver based on silicon and ALN for X-band radar applications. IEEE Trans. Compon. Packag. Manuf. Technol. 2023, 13, 1030–1044.
[21]. Wang, S.; Yan, M.; Chen, H.; Che, W.; Xue, Q. Design of a miniaturized RF front-end module with antenna

array for 5G millimeter-wave communication. In Proceedings of the IEEE International Workshop on Electromagnetics: Applications and Student Innovation Competition (iWEM 2021), Guangzhou, China, 28–30 November 2021; pp. 1–3.

[22]. Fraser, M.; Malladi, V.; Staudinger, J.; Staudinger, J.; Chang, C. A wide-band RF front-end module for 5G MIMO applications. In Proceedings of the IEEE Radio Frequency Integrated Circuits Symposium (RFIC 2020), Los Angeles, CA, USA, 4–6 August 2020; pp. 363–366.

[23]. Kim, Y.; Han, J.; Lee, J.; Jin, T.; Jang, P.; Dhin, H.; Lee, J.; Cho, T. Power-efficient CMOS cellular RF receivers for carrier aggregation according to RF front-end configuration. IEEE Trans. Microw. Theory Tech. 2021, 69, 452–468.

[24]. Liu, T.; Du, B.; Zhong, H.; Wang, H. A carrier aggregation pentaplexer with an optimized phase shifter network in BAW technologies. In Proceedings of the IEEE MTT-S International Microwave Workshop Series on Advanced Materials and Processes for RF and THz Applications (IMWS-AMP 2022), Guangzhou, China, 27–29 November 2022; pp. 1–3.

[25]. Yu, H.; Peng, J.; Wang, X.; Tan, Y.; Wen, P.; Tao, Y.; Deng, L.; Jiang, C. A gold bump flip-chip interconnection structure for face-up MMIC assembly in RF front-end modules. In Proceedings of the IEEE MTT-S International Microwave Workshop Series on Advanced Materials and Processes for RF and THz Applications (IMWS-AMP 2023), Chengdu, China, 13–15 November 2023; pp. 1–3.

[26]. Seo, H.; Zhou, J. Periodically switched acoustic-filtering RF front-ends using commutated-LC circuits for wireless receivers. In Proceedings of the IEEE 22nd Annual Wireless and Microwave Technology Conference (WAMICON 2022), Clearwater, FL, USA, 27–28 April 2022; pp. 1–4.